Optimization of Fiber Ring Resonator Transmission Spectrum Based on Multi-Beam Interference Theory and Transfer Matrix Theory

Wenya Liu, Jiubin Tan, and Jiwen Cui

***Abstract*—Polarization maintaining fiber(PMF) effectively reduces mode splitting and back scattering interference compared to Single Mode Fiber(SMF) in the Fiber Ring Resonator(FRR). In traditional reflection PMF-FRR(RPMF-FRR) structure, classic theoretical model suggests that the orthogonal mode loss difference of the coupler, i.e. the phase difference between the output light field at the cross end and through end of the coupler is $\pi/2$, however, in practical research, this angle is often less than $\pi/2$, which will generate resonance curve asymmetric and severely exacerbate systems instability centered on PMF-FRR. To address this issue, based on the multi-beam interference theory, this article establishes a new mathematical theoretical model and demonstrate a transmission PMF-FRR(TPMF-FRR) with two couplers, the symmetry error has been dwindle to 0.8%, which is a huge improvement compared to 11% of traditional reflection PMF-FRR(RPMF-FRR). Furthermore, different construction methods of TPMF-FRR were studied through theoretical analysis and experimental verification based on the transfer matrix theory, provide guidance for further optimizing the transmission spectrum. The findings contribute to enhance the system precision centered on FRR.**

***Index Terms*—Fiber ring resonator, polarization maintaining fiber, multi-beam interference theory, transfer matrix theory.**

I. Introduction

FIBER ring resonator is an optical resonator formed by enclosing fibers into a closed loop using fiber couplers [1], widely used in fiber lasers [2], [3], optical communicator [4], [5], and fiber sensing [6], [7] due to its simple structure, compact size, stable performance, and ease of integration. PMF-FRR [8] is applied to optimize the FRR transmission spectrum by solving mode splitting and back scattering. However, asymmetric transmission spectrum of FRR has been observed in many researches, results in the inability of the laser center frequency to track and lock the resonant frequency of the FRR, thereby seriously affecting system stability [9]. Prior studies have indicated that including polarization fluctuation [10], Kerr effect [11], temperature disturbance [12], and coupler manufacturing error [13] will affect the symmetry of the resonance curve, of which coupler error is the most influential. Classic theoretical model simply define the orthogonal mode loss difference of the coupler as $\pi/2$, therefore, it can not explain the asymmetry of the resonance curve caused by the RPMF-FRR constructed as the angle is not equal to $\pi/2$, there remains a need of systemic studies to identify the mechanism of asymmetric resonance curve caused by orthogonal mode loss in coupler, and build a structure to enhance the robustness of FRR. In this paper, based on the multi-beam interference theory [14], [15], a model is established to analyze and simulate the asymmetry of the spectrum caused by difference of coupler orthogonal mode loss in the RPMF-FRR and a TPMF-FRR made up of 2 couplers is proposed, the asymmetric error improved from 11% of RPMF-FRR to 0.8% of TPMF-FRR. Furthermore, based on the transfer matrix theory [16], [17], we evaluate different construction methods of FRR using key parameters such as Free Spectrum Range(FSR), Full Width at Half Maximum(FWHM), Fineness(F), and resonant depth(h), both theory and experiment have depict that the fewer segments, the better performance, provided guidance for further optimizing the FRR.

Manuscript received 7 September 2023; revised 18 April 2024; accepted 19 April 2024. Date of publication 23 April 2024; date of current version 2 May 2024. This work was supported by the National Natural Science Foundation of China under Grant 52075131. *(Corresponding author: Jiwen Cui.)*

The authors are with the Key Lab of Ultra-Precision Intelligent Instrumentation, Harbin Institute of Technology, Ministry of Industry and Information Technology, Harbin 150080, China, and also with the Center of Ultra-Precision Optoelectronic Instrument, Harbin Institute of Technology, Harbin 150080, China (e-mail: 21B901002@stu.hit.edu.cn; jbtan@hit.edu.cn; cuijiwen@hit.edu.cn).

Digital Object Identifier 10.1109/JPHOT.2024.3392593

II. Theory and Simulation

To illustrate the issues with traditional models, the influence of PMF-FRR coupler orthogonal loss difference on resonance curve is studied in this section. And we establishes a new mathematical theoretical model and proposed a transmission PMF-FRR(TPMF-FRR) with two couplers based on the theory of multi beam interference, an analysis was conducted on why the structure can eliminate the coupler orthogonal loss difference influence. What's more, different construction methods of TPMF-FRR were studied through theoretical analysis based on the transfer matrix theory.

A. Analysis of the Influence of Coupler Orthogonal Loss Difference

Fig. 1(a) shows the construction of the RPMF-FRR, and the details of light transmission inside the coupler are illustrated in Fig. 1(b). Complex amplitude of each port's optical field signals defined as E_i, where i is the serial number of the port. The output of port 4 is the result of multi beam interference [18]. According to traditional models, in an ideal state, the phase of the light wave will change $\pi/2$ every time it passes through the coupler

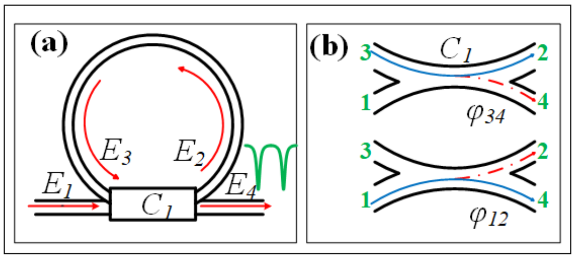

Fig. 1. Structure of PMF-FRR. (a) Structure of RPMF-FRR. (b) Partial enlarged image of coupler C_1.

cross port, and there is no problem caused by the difference in orthogonal mode loss of the coupler. The splitting ratio of the coupler is defined as $k:(1-k)$, the insertion loss of the coupler is p_c and the transmission loss of fiber is p_l, frequency of the input signal is ω, the time for the optical signal to propagate one circle in the FRR is τ. And laser line width is defined as $\triangle\nu$. Therefore, based on classical theory, the output light intensity signal of the RPMF-FRR can be expressed as follows

$$E_2 = \sqrt{p_l}\, e^{-j2\pi\omega\tau}\, e^{-j2\pi\triangle\nu\tau}\, E_3 \tag{1}$$

$$E_3 = e^{j\phi_{13}}\sqrt{(1-k)\,p_c}E_1 + \sqrt{k*p_c}E_2 \tag{2}$$

$$E_4 = \sqrt{kp_c}E_1 + e^{j\phi_{24}}\sqrt{(1-k)\,p_c}E_2 \tag{3}$$

Simultaneous formulas (1) to (3), We can obtain the light intensity signal based on classical theory.

$$\mathrm{I} = \left|\frac{E_4}{E_1}\right|^2 = p_c - \frac{p_c\,(1-k)\left(1-\sqrt{p_cp_l}e^{-4\pi\triangle\nu\tau}\right)}{1+kp_cp_le^{-4\pi\triangle\nu\tau}-2\sqrt{kp_cp_l}e^{-2\pi\triangle\nu\tau}\cos 2\pi\omega\tau} \tag{4}$$

However, due to the difference of coupler orthogonal mode loss, the phase difference of the light between the cross port and the through port will be less than $\pi/2$, resulting in an asymmetric resonance curve. Our hypothesis is the light phase changes ϕ every time it passes through the coupler cross port, the phase changes from Port 1 to Port 3 and from Port 2 to Port 4 are ϕ_{13} and ϕ_{24}, respectively. The light fields output by each port can be represented as:

$$E_2 = \sqrt{p_l}\, e^{-j2\pi\omega\tau}\, e^{-j2\pi\triangle\nu\tau}\, E_3 \tag{5}$$

$$E_3 = e^{j\phi_{13}}\sqrt{(1-k)\,p_c}E_1\sqrt{k*p_c}E_2 \tag{6}$$

$$E_4 = \sqrt{kp_c}E_1 + e^{j\phi_{24}}\sqrt{(1-k)\,p_c}E_2 \tag{7}$$

and the light intensity signal can be written as follows:

$$\mathrm{I} = \left|\frac{E_4}{E_1}\right|^2 = p_ck + p_c\,(1-k) \times \left[\frac{2\sqrt{k}\cos\left(2\pi\omega\tau-\phi_0\right)+\left(1-k-2k\cos\left(\phi_0\right)\right)\sqrt{p}m}{1+kpm^2-2\sqrt{kp}m\cos\left(2\pi\omega\tau\right)}\right] \tag{8}$$

where $m = e^{-2\pi\triangle\nu\tau}$, $p = p_cp_l$, $\phi_0 = \phi_{12}+\phi_{34}$

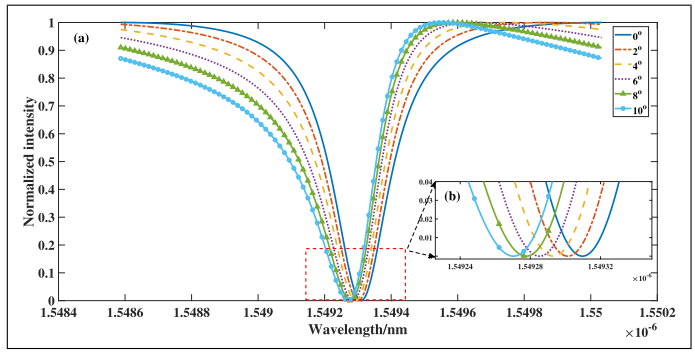

Fig. 2. Resonance curve asymmetric generated by orthogonal loss difference of coupler. (a) Asymmetric resonance curve caused by orthogonal errors of couplers at different angles(0^o to 10^o). (b) Partial enlarged image of resonance curve drift.

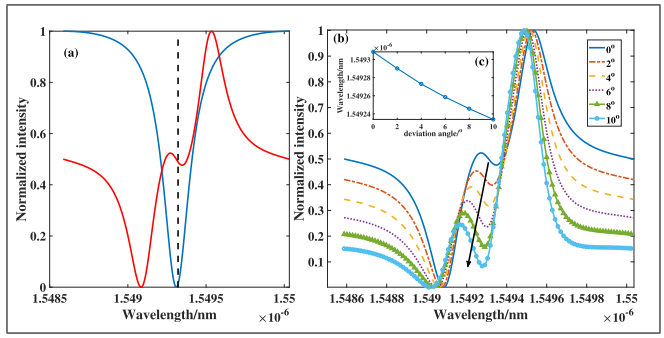

Fig. 3. Demodulation curve asymmetric generated by orthogonal loss difference of coupler. (a) Correspondence between the resonance curve and the demodulation curve. (b) Asymmetric demodulation curve at different angles. (c) The drift of resonance peak caused by different angle errors.

From formula (8), we can see that compared to traditional models, our proposed model takes into account the impact of angle changes, and proves that the resonance curve is influenced by parameter ϕ_0. Fig. 2 displays the simulation results obtained from the preliminary analysis. Compared to the blue resonance curve without error, as the error gradually increases, the symmetry of the resonance curve is gradually disrupted, and the resonance peak gradually drifts, which is plainly shown in Fig. 2(b).

The simulation results validate the previous theoretical analysis that the coupler orthogonal loss difference can cause the resonance curve to drift. Furthermore, we need to analyze the changes of the corresponding demodulation curve when the resonance peak shifts, which is shown in Fig. 3. The resonance peak corresponds to the midpoint of the demodulation curve when there is no error, which is shown in Fig. 3(a). In Fig. 3(b) we can see that the offset of the demodulation curve increases as the coupler error angle increases, as shown by the black arrow in the Fig. 3(b). Furthermore, the relationship between the deviation angle and the deviation wavelength is plotted in the Fig. 3(c). It can be observed that when the deviation angle is 10 degrees, there will be a significant wavelength shift of 0.1 nm. Both theoretical analysis and simulation results indicate that the current model's vague description of phase difference can lead to transmission spectrum drift. Furthermore, in related frequency stabilization

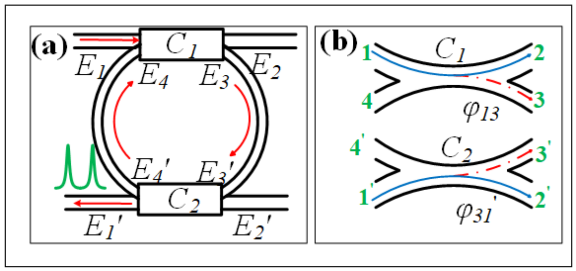

Fig. 4. Structure of PMF-FRR. (a) Structure of RPMF-FRR. (b) Partial enlarged image of coupler C_1.

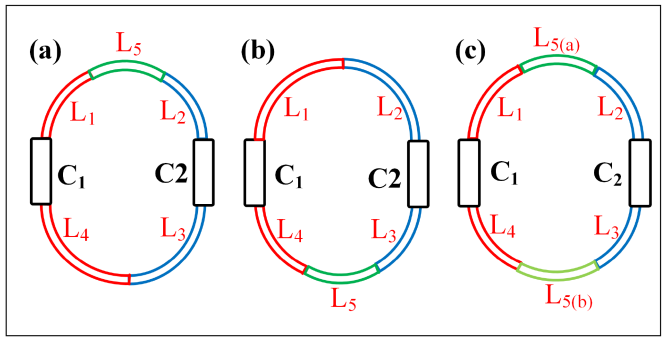

Fig. 5. TPMF-FRR constructed by three methods.

systems and sensing systems based on FRR, accurate frequency locking cannot be achieved, seriously damaging the stability of the system, which is unacceptable in high-precision systems.

B. Analysis of TPMF-FRR Signal Transmission Process

Based on previous theoretical analysis, an error was introduced when the phase change was not strictly equal to $\pi/2$, which will generate resonance curve asymmetric. The traditional model sets the phase as a constant and lacks analysis of phase changes, that is, the structure constructed based on the classical model introduced the error. Although previous work has proposed TPMF-FRR, there is still a scarcity of theoretical analysis and structural design to eliminate resonance curve asymmetric generated by coupler orthogonal difference in this structure. To address the above issues, we intend to use two couplers with the same parameters to form a TPMF-FRR for eliminating the impact of coupler orthogonal loss difference, and to demonstrate this hypothesis based on the theory of multi beam interference. We build a TPMF-FRR and conduct a systematic study on how it can improve the resonance curve asymmetry. Fig. 4(a) shows the structure, which consists of two PM couplers, C1 and C2, the splitting ratios are $k_1 : (1-k_1)$ and $k_2 : (1-k_2)$, the insertion loss are defined as p_{1c} and p_{1c}, the fiber transmission loss is p_{1l} and p_{2l}. Complex amplitude is defined as E_i and E_i', phase changes from Port E_1 to E_3 and from E_3' to E_1' are ϕ_{13} and ϕ_{31}'. Following the previous process, the multiple-beam interference theory was employed to analyze the optical signal transmission process in TPMF-FRR.

$$\mathrm{E}_3 = e^{j\phi_{13}}\sqrt{(1-k_1)\,p_{1c}}E_1 + \sqrt{k_1 p_{1c}}E_4 \tag{9}$$

$$\mathrm{E}_3\prime = \sqrt{p_{1l}}e^{-j2\pi\omega\tau_1}e^{-j2\pi\triangle\nu\tau_1}E_3 \tag{10}$$

$$\mathrm{E}_4\prime = \sqrt{k_2 p_{2c}}E_3\prime \tag{11}$$

$$\mathrm{E}_4 = \sqrt{p_{2l}}e^{-j\omega\tau_2}e^{-2\pi\triangle\nu\tau_2}E_4\prime \tag{12}$$

$$\mathrm{E}_1\prime = e^{j\phi_{13}\prime}\sqrt{(1-k_2)\,p_{2c}}E_3\prime \tag{13}$$

Following the previous process, the optical power is:

$$\mathrm{I} = \left|\frac{E_1\prime}{E_1}\right|^2 = \frac{(1-k_1)\,(1-k_2)\,p_{1c}p_{2c}p_{1l}e^{-4\pi\triangle\nu\tau_1}}{1+kpm^2-2m\sqrt{kp}\cos\left(\tau_1+\tau_2\right)} \tag{14}$$

where $kp = k_{1p}k_{2p}k_{1l}k_{2l}, m = e^{-2\pi\triangle\nu(\tau_1+\tau_2)}$. From the formula (14), it can be seen that the expression for the output optical power does not include phase error, which theoretically proves that TPMF-FRR can solve the problem of asymmetric resonance curves. In the following chapters, we will experimentally verify the improvement of resonance curve asymmetry using the TPMF-FRR constructed based on this theory.

C. Analysis of the Construction Method of TPMF-FRR

Furthermore, this article use the transfer matrix theory to study the different construction methods of TPMF-FRR [19]. Jones matrix is used to build the system models, the attenuation and phase change of the intrinsic light can be obtained by solving the Eigenvalues and eigenvectors, which characterized the suppression of intensity and phase during beam propagation, respectively. However, since the matrix multiplication does not conform to the Commutative property, the transmission matrix constructed based on the three structures shown in Fig. 5 will theoretically generate different eigenvalues and positive vectors. Our hypothesis is the coupling coefficients of coupler C_1 and coupler C_2 are k, so the transfer matrix of the direct transmission port of coupler is:

$$\mathrm{C_t} = \sqrt{10^{-a_c}}\begin{bmatrix}\sqrt{1-k}\cos\theta & -\sqrt{1-k}\sin\theta\\ \sqrt{1-k}\sin\theta & \sqrt{1-k}\cos\theta\end{bmatrix} \tag{15}$$

where θ indicates the coupler polarization axis angle alignment error, and a_k is the loss coefficient. The matrix of PMF can be expressed as:

$$\mathrm{F_{PM}} = \sqrt{10^{\frac{-a_{PM}L_{PM}}{10}}}\begin{bmatrix}e^{-j\beta_{PMx}L_{PM}} & 0\\ 0 & e^{-j\beta_{PMy}L_{PM}}\end{bmatrix} \tag{16}$$

where $a_{PM}, L_{PM}, \beta_{PMx}$ and β_{PMy} are the loss, length and the propagation constant of PMF. And the fiber connection loss is defined as $R = e^{-a_r/2}$. The matrix of light wave for one cycle can be written as:

$$S_1 = C_t \cdot F_{PM1} \cdot R \cdot F_{PM2} \cdot R \cdot F_{PM3} \cdot C_t \cdot F_{PM4} \cdot R \cdot F_{PM5} \tag{17}$$

$$S_2 = C_t \cdot F_{PM1} \cdot R \cdot F_{PM2} \cdot C_t \cdot F_{PM3} \cdot R \cdot F_{PM4} \cdot R \cdot F_{PM5} \tag{18}$$

$$S_3 = C_t \cdot F_{PM1} \cdot R \cdot F_{PM2} \cdot R \cdot F_{PM3} \cdot C_t \cdot F_{PM4} \cdot R \cdot F_{PM5} \cdot R \cdot F_{PM6} \tag{19}$$

TABLE I
ABILITY TO SUPPRESS POLARIZATION NOISE OF THREE FRR

types	$\lambda(1,1)$	$\lambda(2,2)$	I_s
type1	12	0.0014	8571
type2	12	0.0014	8571
type3	3.72	0.0026	1420

Eigenvector $v_{x,m}$, represents the intrinsic polarized light $ESOP_s$ in the FRR, and eigenvalues $\lambda_{x,m}$, phase and mode represent the phase change and intensity loss experienced by the intrinsic polarization state after one cycle of transmission $(x = 1or2; m = 1or2)$, satisfies

$$S_x \cdot v_{x,m} = \lambda_{x,m} \cdot v_{x,m} \tag{20}$$

we need to conduct simulation analysis on the three construction methods based on the results of theoretical analysis, with the main evaluation goal being the ability of the three construction methods to suppress polarization noise. We set $l_i = 0.6$ m, (i = 1, 2, 3, 4, 5), $l_{5a} + l_{5b} = l_5$, $k = 0.5$, $a_R = 0.05$, $a_c = 0.05$, $a_P M = 0.05$, calculating the transfer matrix according to the parameters above and the transfer matrix eigenvalues for three construction structures are:

$$S_{1,2} = \begin{bmatrix} 12 & 0 \\ 0 & 0.0014 + 0.00073i \end{bmatrix} \tag{21}$$

$$S_3 = \begin{bmatrix} 3.72 + 0.05i & 0 \\ 0 & 0.0026 + 0.0009i \end{bmatrix} \tag{22}$$

We define a parameter to evaluate the ability to suppress polarization noise, where:

$$I_s = real\frac{(\lambda(1,1))}{(\lambda(2,2))} \tag{23}$$

indicates intensity suppression. Calculated results are shown in the Table I. It can be found that the three types FRR have strong suppression of polarization noise intensity, but compared to the third one, but the first two construction methods have stronger signal strength, we will also verify the above analysis in the following chapters.

III. EXPERIMENT AND DISCUSSION

In this section, we first established an experimental setup to verify the suppression of mode splitting and backscattering by PMF-FRR, and demonstrated the phenomenon of asymmetric resonance curves. Secondly, based on the theoretical analysis in Section II, a TPMF-FRR was constructed, and its optimization for the asymmetry of the resonance curve was verified through experiments. Finally, based on the transfer matrix theory, we validated the advantages and disadvantages of resonance spectra under different construction methods.

A. Suppressing of Mode Splitting and Backscattering

Fig. 6 shows the experiment setup for obtaining the forward and backward transmission spectrum of FRR. The light emitted from a tunable laser (center wavelength 1550 nm) is first directed to the FRR (SMF or PMF) through port 2 of an fiber Optic circulators, the forward transmission optical signal is converted into

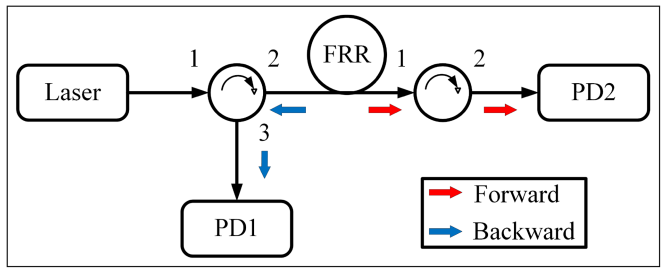

Fig. 6. FRR transmission spectrum detection system.

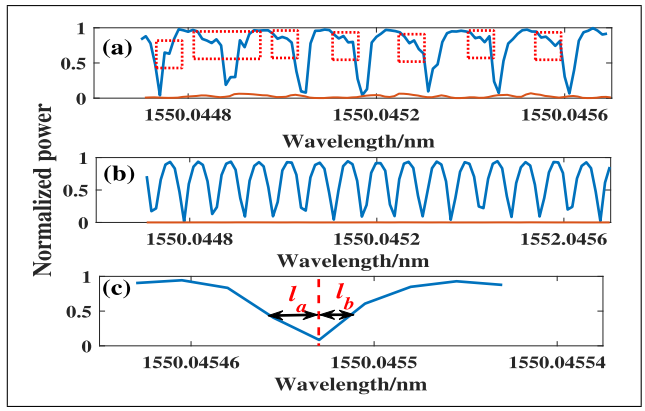

Fig. 7. Spectrum of FRR. (a) Spectrum of SMF-FRR. (b) Spectrum of PMF-FRR. (c) Partial enlarged image of PMF-FRR.

an electric signal by a photo detector(PD), the backward signal was detected by another PD through port 3 of the circulators. The SMF-FRR is composed of an SMF coupler and a two meter long SMF. Correspondingly, the fiber optic devices that make up the same length of PMF-FRR are polarization maintaining. Transmission spectrum are showed in Fig. 7. Fig. 7(a) shows the spectrum of SMF-FRR, due to the inherent fiber loss, the curve is rough and exist many side lobe peaks caused by mode splitting. What's more, the backward signal show in red curve composed of scattered signals and reflected signals is not only an interference, but also, more seriously, it will obstruct the forward signal. Both of these phenomena will result in the laser being unable to track and lock the resonant peak of the resonant cavity, reducing the stability of frequency stabilization or sensing systems centered on SMF-FRR. On the contrary, mode splitting does not exist in PMF-FRR, and the backward signal is too small to affect the forward transmission signal as we can see from Fig. 2(b). However, from Fig. 2(c), we can observe the phenomenon of curve asymmetry of the PMF-FRR. To better evaluate the symmetry of the two structures, a parameter φ is defined as follows,

$$\varphi = \left|\frac{l_a - l_b}{l_a + l_b}\right| \tag{24}$$

where l_a and l_b marked on Fig. 7(c) indicate the absolute distance between the full width at half maxima (FWHM) position coordinate and the trough coordinate, respectively. From Fig. 7, it can be seen that the total length of the FWHM is equal to l_a plus l_b, since the overall length remains largely unchanged, the FWHM

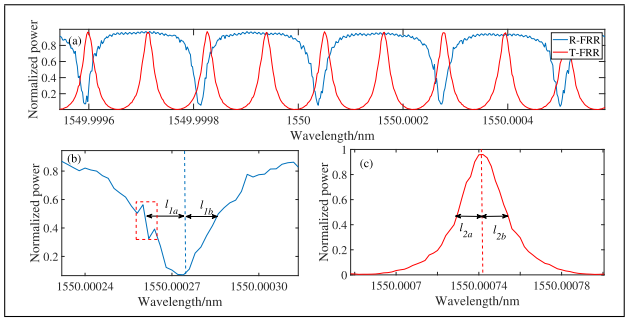

Fig. 8. Transmission spectrum of RPMF-FRR and TPMF-FRR. (a) Transmission spectrum of R-FRR. (b) Transmission spectrum of T-FRR.

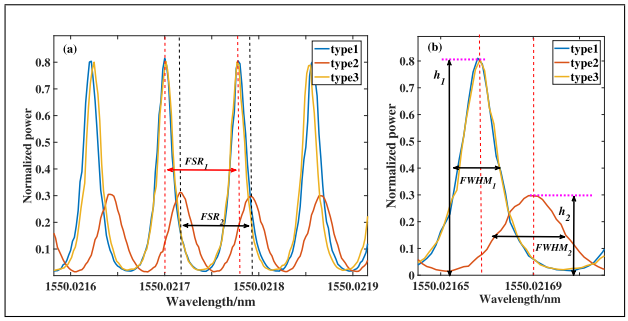

Fig. 9. TPMF-FRR constructed by three methods. (a) TPMF-FRR constructed by three methods. (b) Partial enlarged view.

TABLE II
ASYMMETRY DEGREE φ IN DIFFERENT CONSTRUCTION FORMS

Construction forms	l_a	l_b	φ
RPMF-FRR	8.410	6.745	11%
TPMF-FRR	6.224	6.324	0.8%

TABLE III
COMPARISON OF KEY PARAMETERS

types	FSR/nm	FWHM/nm	F	h
type1	9.615e-5	1.543e-5	6	0.8
type2	9.615e-5	1.543e-5	6	0.79
type3	9.615e-5	3.269e-5	3	0.31

of the FRR constructed according to the proposed scheme in this article is not significantly different from the classical method. However, the classical method simply considers the orthogonal mode loss difference as $\pi/2$ will result the left half length l_a and right half length l_b of FWHM to be unequal, severely disrupting the symmetry of the resonance curve. The scheme proposed in this article can optimize the symmetry of the resonance curve by optimizing the structure of the fiber ring resonator reasonably. In the next section, we will conduct experimental analysis, and the parameterφ will be used to evaluate the symmetry of resonance curves.

B. Suppression of Resonance Curve Asymmetric Generated by Coupler Orthogonal Loss Difference

Prior to the simulation, the expression for the output optical power of TPMF-FRR does not include phase error, compared to traditional PMF-FRR, it eliminates the influence of errors, and experiment was conducted to verify the correctness of the theory. The transmission spectra of TPMF-FRR and RPMF-FRR with the same length of 1 m were displayed in Fig. 8. Partial enlarged images of the transmission spectra of two types FRR are shown in Fig. 8(b) and (c), respectively. Compared to the case where there is significant disturbance in the spectrum of RPMF-FRR, TPMF-FRR is smoother. In order to evaluate the symmetry of the resonance spectra of two types FRR, parameter φ is calculated, as can be seen in Table II.

The parameter φ of R-FRR and T-FRR are 12.9% and 0.8%,respectively, which means the T-FRR can significantly improve the asymmetry as what we have predicted earlier in the paper.

C. Evaluation of Spectral Properties

The experiment results are shown in the Fig. 9. No sidelobe peak in the experimental results proves that all three structures can effectively suppress polarization noise, and the third method has a greater effect on signal attenuation. The experimental results are consistent with the simulation results. As key parameters of the resonance spectrum, Free spectrum range(FSR) [20] and full width at half maximum(FWHM) [21] can be used to describe the resonance curve, furthermore, finesse(F), defined as

$$F = \frac{FSR}{FWHM} \tag{25}$$

and resonance depth, can evaluate the quality of the resonant cavity, since the larger these two parameters, the more energy is coupled into the resonant cavity [22]. Analyze the results marked in the Fig. 9(a) and (b), and the comparison results are shown in the Table III.

The results indicate that due to the same length, the FSR of three type are same. About the F and the resonance depth, the first two FRRs are very close without changing the parameters of the coupler and polarization maintaining fiber, however, due to the increased complexity of the structure, the precision and resonance depth of the third type of FRR are severely attenuated, accounting for 50% and 60% of the first two, respectively. This indicates that energy is not fully coupled into the resonant cavity, which is exactly what high-precision sensing systems built centered the FRR do not expect.

IV. CONCLUSION

In conclusion, classic theoretical model simply define the orthogonal mode loss difference of the coupler as $\pi/2$, which makes it impossible to describe the asymmetric phenomenon of the resonance curve and will severely exacerbate systems instability centered on PMF-FRR. To address this issue, based on the multi-beam interference theory, this article establishes a new mathematical theoretical model and demonstrate a transmission PMF-FRR(TPMF-FRR) with two couplers, fill the gap in theory. Experiments have shown that compared to traditional SMF-FRR, the asymmetry parameter has been improved from the original 11% to 0.7%. Based on transmission matrix theory, We analyzed the impact of different construction methods on

FRR transmission spectrum. Simulation and experimental results show that, under a certain length, the fewer fiber segments, the stronger the suppression of polarization noise, and the higher the resonance depth and fineness of the spectrum, this is what high precision frequency stabilization system and sensing system need, the outcomes of this study are expected to optimize the system centered as FRR.

REFERENCES

[1] S. Wang, H. Pi, Y. Feng, and J. Yan, "Optical mode localization sensing based on fiber-coupled ring resonators," *Opt. Exp.*, vol. 31, no. 13, pp. 21834–21844, Jun. 2023.

[2] J. He, B. Xu, X. Xu, C. Liao, and Y. Wang, "Review of femtosecond-laser-inscribed fiber Bragg gratings: Fabrication technologies and sensing applications," *Photon. Sensors*, vol. 11, no. 2, pp. 203–226, Jun. 2021.

[3] P. Grelu and N. Akhmediev, "Dissipative solitons for mode-locked lasers," *Nature Photon.*, vol. 6, no. 2, pp. 84–92, Feb. 2012.

[4] B. J. Puttnam, G. Rademacher, and R. S. Luis, "Space-division multiplexing for optical fiber communications," *Optica*, vol. 8, no. 9, pp. 1186–1203, Sep. 2021.

[5] J. Zhao, J. Du, Y. Yue, and J. Liu, "Special issue on advanced technique and future perspective for next generation optical fiber communications," *Photonics*, vol. 9, no. 5, May 2022, Art. no. 280.

[6] P. Lu et al., "Distributed optical fiber sensing: Review and perspective," *Appl. Phys. Rev.*, vol. 6, no. 4, Dec. 2019, Art. no. 041302.

[7] T. Liu, Y. Chen, Q. Han, and X. Lü, "Magnetic field sensor based on U-bent single-mode fiber and magnetic fluid," *IEEE Photon., J.*, vol. 6, no. 6, Dec. 2014, Art. no. 5300307.

[8] S. Sun et al., "Polarization-maintaining terahertz anti-resonant fibers based on mode couplings between core and cladding," *Results Phys.*, vol. 25, Jun. 2021, Art. no. 104309.

[9] D. Song, K. Yin, S. Kong, X. Chen, and Z. Xu, "Theoretical and experimental investigations of tunable microwave signal generation based on a 1-GHz all-polarization-maintaining mode-locked fiber laser," *Photonics*, vol. 9, no. 10, Oct. 2022, Art. no. 717.

[10] D. Xu, O. Lopez, A. Amy-Klein, and P.-E. Pottie, "Polarization scramblers to solve practical limitations of frequency transfer," *J. Lightw. Technol.*, vol. 39, no. 10, pp. 3106–3111, May 2021.

[11] N. Moroney et al., "A kerr polarization controller," *Nature Commun.*, vol. 13, no. 1, Jan. 2022, Art. no. 398.

[12] J. Hu et al., "Influence of Kerr nonlinearity on propagation characteristics of twisted Gaussian Schell-model beams," *Opt. Exp.*, vol. 29, no. 15, pp. 23393–23407, Jul. 2021.

[13] F. Yu et al., "Resetting directional couplers for high-fidelity quantum photonic integrated chips," *Opt. Lett.*, vol. 46, no. 20, pp. 5181–5184, Oct. 2021.

[14] F. Wen et al., "Terahertz tunable optically induced lattice in the magnetized monolayer graphene," *Opt. Exp.*, vol. 30, no. 2, pp. 2852–2862, Jan. 2022, doi: 10.1364/OE.448926.

[15] X. Wang, L. Feng, J. Xu, and P. Ni, "Steady-state frequency-tracking distortion in the digital Pound-Drever-Hall technique," *Appl. Opt.*, vol. 59, no. 5, pp. 1347–1352, Feb. 2020.

[16] B. S. Dias et al., "Refractometric sensitivity of Bloch surface waves: Perturbation theory calculation and experimental validation," *Opt. Lett.*, vol. 48, no. 3, pp. 727–730, Feb. 2023.

[17] V. Gasparic, T. G. Mayerhoefer, D. Zopf, D. Ristic, J. Popp, and M. Ivanda, "To generate a photonic nanojet outside a high refractive index microsphere illuminated by a gaussian beam," *Opt. Lett.*, vol. 47, no. 10, pp. 2534–2537, May 2022, doi: 10.1364/OL.459001.

[18] X. He, D. Liu, and J. Zhou, "Volume hologram–coupled Fabry-Perot etalon," *Optik*, vol. 114, no. 8, pp. 379–383, 2003, doi: 10.1078/0030-4026-00278.

[19] Y. Zeng, Z.-X. Ling, G.-D. Liu, L.-L. Wang, and Q. Lin, "Tunable plasmonically induced transparency with giant group delay in gain-assisted graphene metamaterials," *Opt. Exp.*, vol. 30, no. 9, pp. 14103–14111, Apr. 2022, doi: 10.1364/OE.455954.

[20] B. Zhang et al., "Advancing aluminum casting optimization with real-time temperature and gap measurements using optical fiber sensors at the metal-mold interface," *IEEE Trans. Instrum. Meas.*, vol. 72, 2023, Art. no. 7008412, doi: 10.1109/TIM.2023.3329217.

[21] M. W. Puckett et al., "422 million intrinsic quality factor planar integrated all-waveguide resonator with sub-MHz linewidth," *Nature Commun.*, vol. 12, no. 1, Feb. 2021, Art. no. 934, doi: 10.1038/s41467-021-21205-4.

[22] S. Yuan et al., "On-chip terahertz isolator with ultrahigh isolation ratios," *Nature Commun.*, vol. 12, no. 1, Sep. 2021, Art. no. 5570, doi: 10.1038/s41467-021-25881-0.